Advances in Difference Equations
a SpringerOpen Journal

RESEARCH Open Access

Analyzing transient response of the parallel RCL circuit by using the Caputo–Fabrizio fractional derivative

Shahram Alizadeh[1], Dumitru Baleanu[2,3] and Shahram Rezapour[1*]

*Correspondence:
rezapourshahram@yahoo.ca
[1]Department of Mathematics, Azarbaijan Shahid Madani University, Tabriz, Iran
Full list of author information is available at the end of the article

Abstract

In this paper, the transient response of the parallel RCL circuit with Caputo–Fabrizio derivative is solved by Laplace transforms. Also, the graphs of the obtained solutions for the different orders of the fractional derivatives are compared with each other and with the usual solutions. Finally, they are compared with practical and laboratory results.

MSC: Primary 34A08; secondary 34A12

Keywords: Caputo–Fabrizio derivative; Fractional differential; Transient response

1 Introduction

The idea of fractional calculus coincides with that of classical calculus. Leibniz and l'Hopital first raised this issue in 1695 and in 1730 Euler's attention was drawn to it, followed by Lagrange in 1772 and Laplace in 1812. The first concept of arbitrary derivation was introduced by Lacroix and later by Fourier, Abel, Liouville, Grunewald, Letnikov and Riemann. Various fractional derivatives were thus introduced. Grunewald and Krug introduced the work of Riemann and Liouville and introduced another integral and derivative called Riemann–Liouville. Caputo introduced a new derivative by rewriting the Riemann–Liouville formula. In 2014, the conformable derivative was introduced, which was in fact a generalization of the classical derivative and so far, many researchers have used them [13, 22, 25, 31, 32]. In 2015 Caputo and Fabrizio introduced a new fractional derivative using the exponential function. This derivative has no singularity [20] and [36]. In [4] the derivative properties of Caputo–Fabrizio were developed by Atangana. In [5] the advantages of the new differential operators are explained. Following this same process, Atangana and Baleanu introduced another derivative of Caputo–Fabrizio by introducing the Mittag-Leffler function into the fractional derivative, which many researchers have used in their papers. Many important discussions are presented in [7] and [8]. New extensions and generalizations of the Caputo–Fabrizio derivative and other fractional derivatives can be found in articles [10, 11, 14–16]. New entries in other areas of fractional calculus are presented in articles [1, 2, 12, 17, 18, 23, 35]. In this paper, we will investigate the parallel RCL circuit with the Caputo–Fabrizio fractional derivative.

© The Author(s) 2020. This article is licensed under a Creative Commons Attribution 4.0 International License, which permits use, sharing, adaptation, distribution and reproduction in any medium or format, as long as you give appropriate credit to the original author(s) and the source, provide a link to the Creative Commons licence, and indicate if changes were made. The images or other third party material in this article are included in the article's Creative Commons licence, unless indicated otherwise in a credit line to the material. If material is not included in the article's Creative Commons licence and your intended use is not permitted by statutory regulation or exceeds the permitted use, you will need to obtain permission directly from the copyright holder. To view a copy of this licence, visit http://creativecommons.org/licenses/by/4.0/.

A circuit including resistance, capacitor and inductor RCL is an important circuit which is used in most electronic devices. By considering the importance of this circuit, we are going to examine the transient response of parallel RCL circuit with the Caputo–Fabrizio derivative. The RCL, RL, RC and LC series circuits with Caputo–Fabrizio and other fractional derivative have already been examined by some researchers like in [3, 6, 9, 19, 21, 24, 26–28, 31, 34, 37, 38].

First, we provide some basic notions as regards the Caputo–Fabrizio derivative. Let $0 < \alpha < 1$ and $f \in H^1(a,b)$. The Caputo–Fabrizio derivative is defined by

$$\mathcal{D}_t^{(\alpha)} f(t) = \frac{M(\alpha)}{(1-\alpha)} \int_0^t f'(s) \exp\left(-\frac{\alpha}{1-\alpha} t\right) ds,$$

where $M(\alpha)$ is a normalization function such that $M(0) = M(1) = 1$ [20]. For $n \geq 1$, the Caputo–Fabrizio derivative of order $n+\alpha$ is defined by $\mathcal{D}_t^{(\alpha+n)} f(t) = \mathcal{D}_t^{(\alpha)}(\mathcal{D}_t^{(n)} f(t))$ and the Laplace transform of the Caputo–Fabrizio derivative is defined by

$$\begin{aligned}\mathcal{L}\left[\mathcal{D}_t^{(\alpha)} f(t)\right] &= \frac{1}{1-\alpha} \int_0^\infty \exp(-st) \int_0^t f'(\tau) \exp\left(-\frac{\alpha(t-\tau)}{1-\alpha}\right) d\tau\, dt \\ &= \frac{1}{1-\alpha} \mathcal{L}\left[f'(t)\right] \mathcal{L}\left[\exp\left(-\frac{\alpha t}{1-\alpha}\right)\right].\end{aligned}$$

Then we have $\mathcal{L}[\mathcal{D}_t^{(\alpha)} f(t)] = \frac{s\mathcal{L}[f(t)]-f(0)}{s+\alpha(1-s)}$,

$$\mathcal{L}\left[\mathcal{D}_t^{(\alpha+1)} f(t)\right] = \frac{1}{1-\alpha} \mathcal{L}\left[f''(t)\right] \mathcal{L}\left[\exp\left(-\frac{\alpha t}{1-\alpha}\right)\right] = \frac{s^2 \mathcal{L}[f(t)] - sf(0) - f'(0)}{s + \alpha(1-s)},$$

and

$$\begin{aligned}\mathcal{L}\left[\mathcal{D}_t^{(\alpha+n)} f(t)\right] &= \frac{1}{1-\alpha} \mathcal{L}\left[f^{(n+1)}(t)\right] \mathcal{L}\left[\exp\left(-\frac{\alpha t}{1-\alpha}\right)\right] \\ &= \frac{s^{n+1} \mathcal{L}[f(t)] - s^n f(0) - s^{n-1} f'(0) - \cdots - f^{(n)}(0)}{s + \alpha(1-s)}.\end{aligned}$$

Finally, the fractional integral of order α is defined by $I^\alpha f(t) = (1-\alpha) f(t) + \alpha \int_0^t f(s)\, ds$ [36].

2 RCL circuit

The RCL circuit is used frequently in many branches of science such as computer science and electronics. We know that boost circuits and bucks are used in power supply of op and amp circuits, cpu's etc. According to Ohm's law, the voltage of the conductor is proportional to the intensity of the current it passes through. The mathematical formula can be written $V(t) = RI(t)$, where $I(t)$ is the current flowing through the conductor measured in ampère (A), $V(t)$ is the potential difference measured between two points of the conductor in units of volts (V) and R is the resistance of the conductor measured in [Ohm] (Ω). The change in the charge q with respect to time t is $I(t) = \frac{dq}{dt}$. Thus, Ohm's law can be written as $V(t) = R\frac{dq}{dt}$. Now we use the fractional time derivative operator

$$\frac{d^\alpha}{dt^\alpha} := \mathcal{D}_t^{(\alpha)} \quad (0 \leq \alpha < 1) \tag{1}$$

where α is an accord parameter close to 1, which represents the order of the derivative and in the case $\alpha = 1$ it becomes the ordinary derivative operator [30]. However, the ordinary time operator has dimensions of inverse second $[\frac{1}{s}]$ [30], while Eq. (1) has dimension $[\mathcal{D}_t^{(\alpha)}] = \frac{1}{s^\alpha}$. Thus, it is different from the ordinary time derivative. There has been introduced a new parameter σ by

$$\left[\frac{1}{\sigma^{1-\alpha}}\mathcal{D}_t^{(\alpha)}\right] = \frac{1}{s} \quad (0 \le \alpha < 1) \tag{2}$$

such that, for the case $\alpha = 1$, Eq. (2) becomes an ordinary derivative [30]. This is true if the parameter σ has the dimensions $[\sigma] = s$ [30]. Therefore, we can change the ordinary time derivative operator by $\frac{d}{dt} \to \frac{1}{\sigma^{1-\alpha}}\mathcal{D}_t^{(\alpha)}$ and $\frac{d^2}{dt^2} \to \frac{1}{\sigma^{2(1-\alpha)}}\mathcal{D}_t^{(2\alpha)}$, where $n-1 \le \alpha < n$. By using these expressions, Ohm's law becomes the fractional Ohm law, $V(t) = R \times \frac{1}{\sigma^{1-\alpha}}\mathcal{D}_t^{(\alpha)}q(t)$. Since the energy can be stored in the capacitor and inductor, the primary inductor current and primary capacitor voltage both can be non-zero. Consider Figs. 1 and 2.

In Fig. 2, similar to [33], we can use Kirchhoff's law (KCL) as

$$\frac{V}{R} + \frac{1}{L}\int_{t_0}^{t} V\,dt - i(t_0) + C\frac{dV}{dt} = 0, \tag{3}$$

where $I(0) = I_0$ and $V(0) = V_0$. If we use normal derivative for (3), then we obtain the following differential equation:

$$C\frac{d^2V}{dt^2} + \frac{1}{R}\frac{dV}{dt} + \frac{1}{L}V = 0. \tag{4}$$

Figure 1 RCL circuit with battery and switch is open

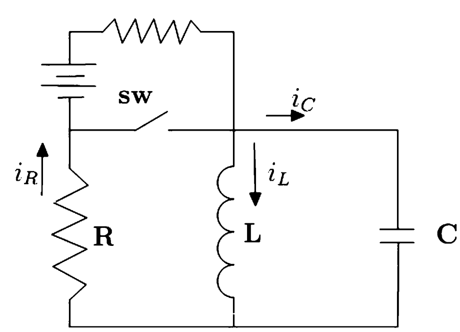

Figure 2 RCL circuit after switch is closed

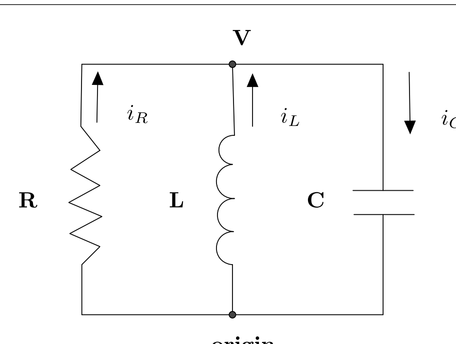

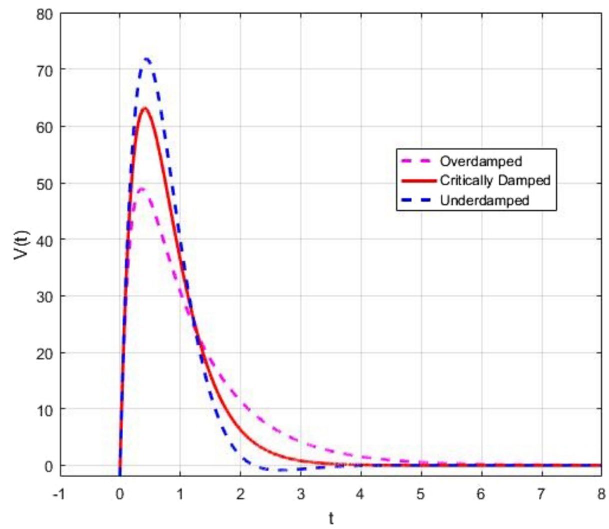

Figure 3 Graph of transient response in overdamped, critically damped and underdamped case

Note that its solution is a natural response of the circuit which we need. For solving Eq. (4) with normal derivative, we consider three cases. In this way, put $a = \frac{1}{2RC}$ and $\omega_0 = \frac{1}{\sqrt{LC}}$. Note that, for avoiding computations in numerical examples, non-laboratory inductor and capacitor values have been selected by researchers usually.

The overdamped case concerns $a > \omega_0$.

In this case, the transient response of the circuit has the form $V(t) = A_1 e^{s_1 t} + A_2 e^{s_2 t}$, where $s_1 = -a + \sqrt{a^2 - \omega_0^2}$ and $s_2 = -a - \sqrt{a^2 - \omega_0^2}$. For example put $R = 6\ \Omega$, $C = \frac{1}{42}$ F and $L = 7$ H. Then we get $s_1 = -1$ and $s_2 = -6$. Hence, $V(t) = A_1 e^{-t} + A_2 e^{-6t}$. Thus, $V(0) = A_1 + A_2 = 0$ and $\frac{dV}{dt}|_{t=0} = -A_1 - 6A_2$. Since the voltage of the resistor is zero at $t = 0$, we have $i_R(0) = 0$ and $\frac{dV}{dt}|_{t=0} = \frac{i_C(0)}{C} = \frac{I(0)+i_R(0)}{C} = \frac{I(0)}{C} = 420(V/S)$ and so $A_1 = 84$ and $A_2 = -84$. Hence, $V(t) = 84e^{-t} - 84e^{-6t}$.

The critically damped case concerns $a = \omega_0$.

In this case the response has the form $V(t) = (A_1 + A_2 t)e^{-at}$. For example put $R = 8.57\ \Omega$, $C = \frac{1}{42}$ F, $L = 7$ H, $i(0) = 10$ A and $V(0) = 0$. Then we have $V(t) = 420te^{-\sqrt{6}t}$.

The underdamped case concerns $a < \omega_0$.

In this case the roots of the characteristic equation are complex and may be expressed as $s_{1,2} = a \pm j\omega_d$, where $\omega_d = \sqrt{\omega_0^2 - a^2}$ and $j = \sqrt{-1}$. In this case, the transient response of the circuit has the form $V(t) = e^{-at}(A_1 \cos \omega_d t + A_2 \sin \omega_d t)$. For example put $R = 10.5\ \Omega$, $C = \frac{1}{42}$ F, $L = 7$ H, $i(0) = 10$ A and $V(0) = 0$. Then we have $V(t) = 210\sqrt{2}e^{-2t}\sin(\sqrt{2}t)$. Check Fig. 3 and compare the cases.

3 Main result

Now by Eq. (4) and changing the ordinary time derivative operator by $\frac{d}{dt} \to \frac{1}{\sigma^{1-\alpha}}\mathcal{D}_t^{(\alpha)}$ and $\frac{d^2}{dt^2} \to \frac{1}{\sigma^{2(1-\alpha)}}\mathcal{D}_t^{(2\alpha)}$, we obtain the following equation

$$\frac{1}{\sigma^{2(1-\alpha)}}\mathcal{D}_t^{(2\alpha)}V(t) + \frac{1}{RC\sigma^{(1-\alpha)}}\mathcal{D}_t^{(\alpha)}V(t) + \frac{1}{LC}V(t) = 0. \tag{5}$$

For simplicity, put $A = \frac{\sigma^{(1-\alpha)}}{RC}$ and $B = \frac{\sigma^{2(1-\alpha)}}{LC}$. Thus, we have

$$\mathcal{D}_t^{(2\alpha)}V(t) + A\mathcal{D}_t^{(\alpha)}V(t) + BV(t) = 0. \tag{6}$$

We suppose in Fig. 2 that only the inductor has primary energy, that is, $V(t_0) = V(0) = 0$. Now, put $U(t) = \mathcal{D}_t^{(\alpha)}V(t)$. Thus, $\mathcal{D}_t^{(2\alpha)}V(t) = \mathcal{D}_t^{(\alpha)}U(t)$ and so

$$\begin{aligned}\mathcal{L}\big[\mathcal{D}_t^{(2\alpha)}V(t)\big] &= \mathcal{L}\big[\mathcal{D}_t^{(\alpha)}\big(\mathcal{D}_t^{(\alpha)}V(t)\big)\big] = \mathcal{L}\big[\mathcal{D}_t^{(\alpha)}\big(U(t)\big)\big] \\ &= \frac{s\mathcal{L}[U(t)] - U(0)}{s+\alpha(1-s)} = \frac{s\mathcal{L}[U(t)]}{s+\alpha(1-s)}.\end{aligned} \tag{7}$$

Note that $U(0) = \frac{M(\alpha)}{1-\alpha}\int_0^0 V'(t)\exp(-\frac{\alpha(t-x)}{1-\alpha})dx = 0$ and

$$\mathcal{L}\big[U(t)\big] = \frac{s\mathcal{L}[V(t)] - V(0)}{s+\alpha(1-s)} = \frac{s\mathcal{L}[V(t)]}{s+\alpha(1-s)}. \tag{8}$$

Thus, by using (7) and (8) we get $\mathcal{L}[\mathcal{D}_t^{(2\alpha)}V(t)] = \frac{s^2\mathcal{L}[V(t)]}{(s+\alpha(1-s))^2}$. Now by applying the Laplace transform on both sides of (6), we obtain $\frac{s^2\mathcal{L}[V(t)]}{(s+\alpha(1-s))^2} + A\frac{s\mathcal{L}[V(t)]}{(s+\alpha(1-s))} + B\mathcal{L}[V(t)] = 0$ and $\mathcal{L}[V(t)](\frac{s^2}{(s+\alpha(1-s))^2} + \frac{As}{(s+\alpha(1-s))} + B) = 0$. Hence, $\mathcal{L}[V(t)](\frac{s^2+As(s+\alpha(1-s))+B(s+\alpha(1-s))^2}{(s+\alpha(1-s))^2}) = 0$. If $\mathcal{L}[V(t)] = 0$, then $V(t) = 0$ is an obvious solution for Eq. (6). Thus, we should have $s^2 + A(s^2 + \alpha s(1-s)) + B(s+\alpha(1-s))^2 = 0$ and so

$$\big(1 + A(1-\alpha) + B(1-\alpha)^2\big)s^2 + \alpha\big(A + 2B(1-\alpha)\big)s + B\alpha^2 = 0.$$

Thus, $s_1, s_2 = \frac{-(\alpha(A+2B(1-\alpha)))\pm[(\alpha(A+2B(1-\alpha)))^2-4(1+A(1-\alpha)+B(1-\alpha)^2)(B\alpha^2)]^{\frac{1}{2}}}{2(1+A(1-\alpha)+B(1-\alpha)^2)}$. Hence, we obtain the solution. For example, let $R = 6\ \Omega$, $L = 7$ H, $I(0) = 10A$, $V(0) = 0$, $C = \frac{1}{42}$ F, $\alpha = 1$ and σ be a non-negative constant. Then we have $A = \frac{\sigma^{(1-\alpha)}}{RC} = 7$, $B = \frac{\sigma^{2(1-\alpha)}}{LC} = 6$, $s_1 = -1$ and $s_2 = -6$. Thus, the transient response of Eq. (5) for $\alpha = 1$ is equal to the transient response of Eq. (4) and we have

$$V(t) = 84e^{-t} - 84e^{-6t}. \tag{9}$$

In Figs. 4(a) and 4(b), we observe the graph of (9) for $\sigma = \frac{1}{4}, \frac{1}{2}, \frac{3}{4}, 1, \frac{5}{4}$ and $\alpha = \frac{1}{4}, \frac{1}{2}, \frac{3}{4}, 1$. It is clear that the graphs of (9) for $\alpha = 1$ and each σ are the same.

Now suppose in Fig. 1 the inductor and the capacitor both have primary energy. Then we get $V(0) \neq 0$ and

$$\mathcal{L}\big[\mathcal{D}_t^{(2\alpha)}V(t)\big] = \frac{s^2\mathcal{L}[V(t)] - sV(0)}{(s+\alpha(1-s))^2} \tag{10}$$

and so Eq. (6) gets the form

$$\frac{s^2\mathcal{L}[V(t)] - sV(0)}{(s+\alpha(1-s))^2} + A\frac{s\mathcal{L}[V(t)] - V(0)}{(s+\alpha(1-s))} + B\mathcal{L}\big[V(t)\big] = 0 \tag{11}$$

and from the above equation we have

$$s^2\mathcal{L}\big[V(t)\big] - sV(0) + A\big(s+\alpha(1-s)\big)\big[s\mathcal{L}\big[V(t)\big] - V(0)\big] + B\big(s+\alpha(1-s)\big)^2\mathcal{L}\big[V(t)\big] = 0;$$

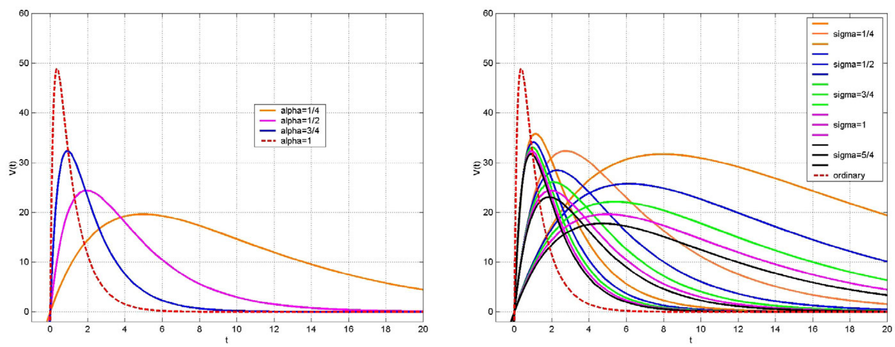

(a) $\sigma = 1$ (b) $\alpha = 1/4, 1/2, 3/4, 1$

Figure 4 Graphs of Eq. (9) with selected α and σ values

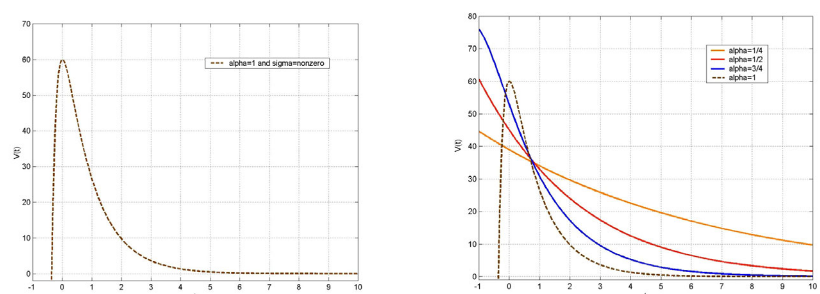

(a) Graph of Eq. (13 with $\alpha = 1$ and $\sigma = non-zero$ (b) Graphs of Eq. (13 with $\sigma = 1$ and selected α values.

Figure 5 Graphs of Eq. (13) with $L = 7$ H, $R = 6\ \Omega$, $C = \frac{1}{42}$ F

then

$$\mathcal{L}\big[V(t)\big]\big(s^2 + As\big(s + \alpha(1-s)\big) + B\big(s + \alpha(1-s)\big)^2\big) = sV(0) + A\big(s + \alpha(1-s)\big)V(0)$$

and

$$\mathcal{L}\big[V(t)\big] = \frac{sV(0) + A(s + \alpha(1-s))V(0)}{s^2 + As(s + \alpha(1-s)) + B(s + \alpha(1-s))^2)}. \qquad (12)$$

By the inverse Laplace transform we have

$$V(t) = \mathcal{L}^{-1}\left[\frac{sV(0) + A(s + \alpha(1-s))V(0)}{s^2 + As(s + \alpha(1-s)) + B(s + \alpha(1-s))^2)}\right]. \qquad (13)$$

In the following we consider the graph of Eq. (13) in Fig. 5(a) with $\sigma = 1$ and $\alpha = 1$ and (b) with $\sigma = 1$ and $\alpha = 1/4, 1/2, 3/4, 1$. Figure 6 shows the graphs of Eq. (13) with $L = 7$ H, $R = 6\ \Omega$, $C = \frac{1}{42}$ F, $\alpha = 1/4, 1/2, 3/4, 1$ and $\sigma = 1/4, 1/2, 3/4, 1$.

Now we want to study the graph of voltage function on the capacitor when the switch is on in Fig. 7.

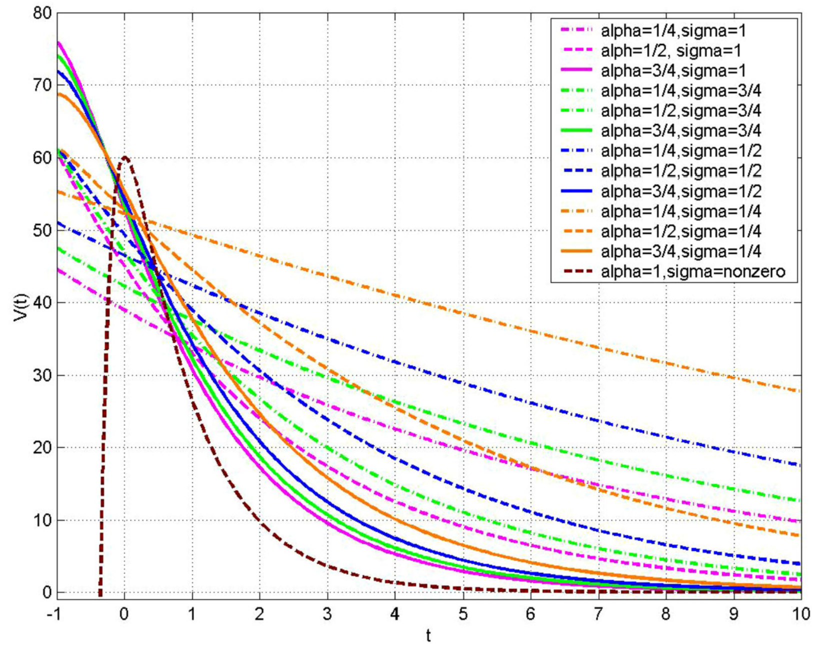

Figure 6 Graphs of Eq. (13) with $L = 7$ H, $R = 6\ \Omega$, $C = \frac{1}{42}$ F

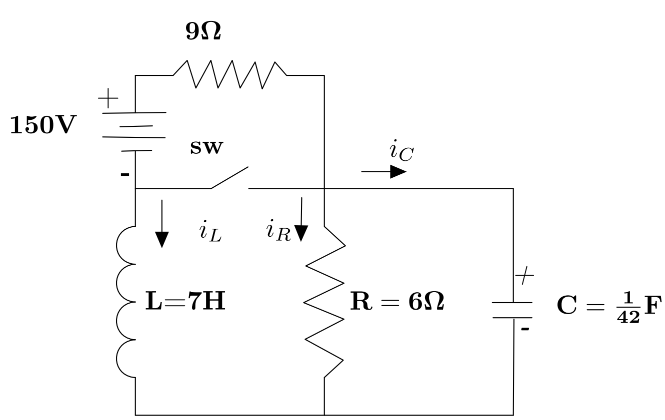

Figure 7 RCL circuit

Thus for $L = 7$ H, $R = 6\ \Omega$ and $C = \frac{1}{42}$ F we have

$$a = \frac{1}{2RC} = 3.5\left(\frac{1}{s}\right) \quad \text{and} \quad \omega_0 = \frac{1}{\sqrt{LC}} = \sqrt{6}\left(\frac{rad}{s}\right)$$

and $s_1 = -1(\frac{1}{s})$ and $s_2 = -6(\frac{1}{s})$ so the total solution is

$$V(t) = A_1 \exp^{-t} + A_2 \exp^{-6t}. \tag{14}$$

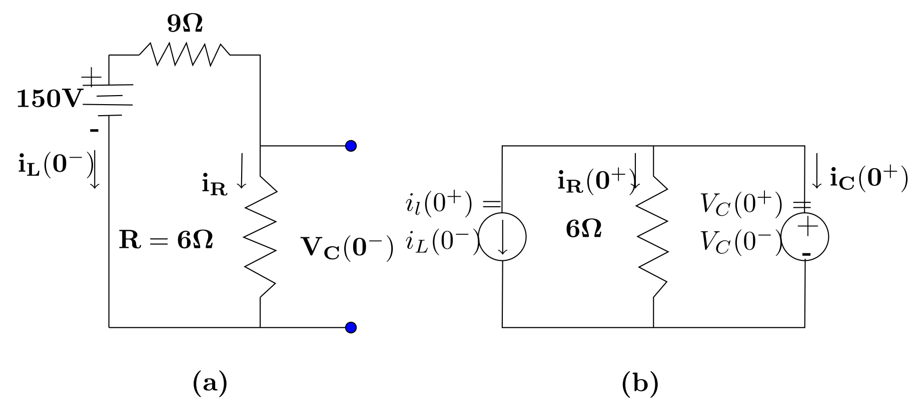

Figure 8 RCL circuit with switch off and on

We suppose that the switch has been turned up during $0^- < t < 0^+$ and we isolate the voltage source and resistance (9 Ω) from the circuit. We must calculate $V_c(0^+)$ and $\frac{dV_C}{dt}|_{t=0^+}$, and to do this we need Fig. 8.

In Fig. 8(a) $t = 0^-$ and in Fig. 8(b) $t = 0^+$ so in Fig. 8(a) we have

$$I_L\left(0^-\right) = \frac{-150}{6+9} = -10 \text{ A}, \qquad V_C\left(0^-\right) = 6 \times (10) = 60 \text{ V},$$

and

$$\left.\frac{dV_C}{dt}\right|_{t=0^+} = \frac{1}{C} I_C\left(0^+\right) = \frac{1}{C}\left(-I_C\left(0^+\right) - I_R\left(0^+\right)\right) = 42\left(10 - \frac{60}{6}\right) = 0;$$

now set this values to $V_C(t)$ and $\frac{dV_C}{dt}|_{t=0^+}$ in $t = 0^+$, then from (14) we have

$$V_C\left(0^+\right) = 60 = A_1 + A_2, \qquad \left.\frac{dV_C}{dt}\right|_{t=0^+} = 0 = -A_1 - 6A_2, \quad t > 0,$$

so $A_2 = -12$ and $A_1 = 72$ and thus

$$V_C(t) = 72 \exp^{-t} - 12 \exp^{-6t}, \quad t > 0. \tag{15}$$

In Fig. 9 the graph of Eq. (15) is considered.

So Eq. (13) with $\alpha = 1$ and σ = non-zero is equal to Eq. (15).

Now we return to Eq. (3) and try to solve it in three cases.

Case 1: apply the Laplace transform to both sides of (3):

$$\begin{aligned}
&\mathcal{L}\left[\frac{V}{R} + \frac{1}{L}\int_0^t V(p)\,dp - I(0) + C\frac{dV}{dt}\right] = 0, \\
&\frac{1}{R}\mathcal{L}\left[V(t)\right] + \frac{1}{Ls}\mathcal{L}\left[V(t)\right] - \frac{I(0)}{s} + C\left(s\mathcal{L}\left[V(t)\right] - V(0)\right) = 0, \\
&\mathcal{L}\left[V(t)\right]\left(\frac{1}{R} + \frac{1}{Ls} + Cs\right) = \frac{I(0)}{s} + CV(0), \\
&\mathcal{L}\left[V(t)\right] = \frac{\frac{I(0)}{s} + CV(0)}{\frac{1}{R} + \frac{1}{Ls} + Cs},
\end{aligned}$$

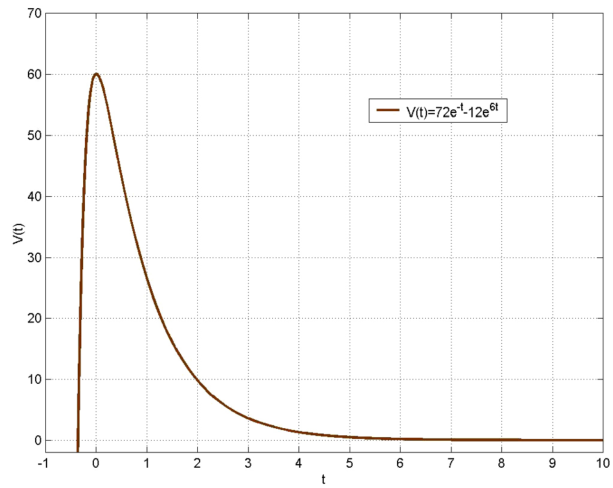

Figure 9 Graph of Eq. (15)

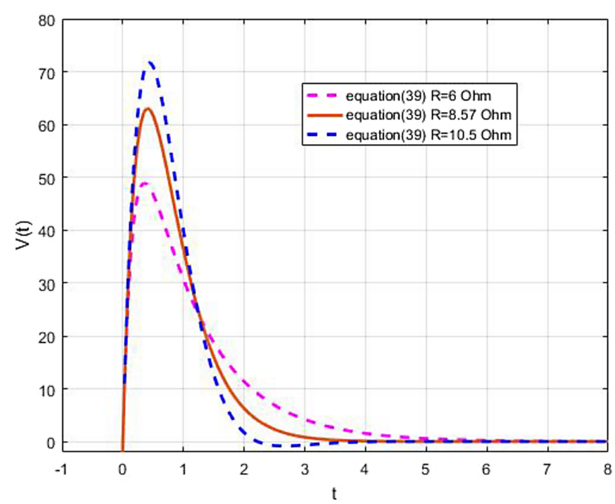

Figure 10 Graph of Eq. (16) with $V(0) = 0$, $L = 7$ H, $I(0) = 10$ A, $C = \frac{1}{42}$ F

$$V(t) = \mathcal{L}^{-1}\left[\frac{\frac{I(0)}{s} + CV(0)}{\frac{1}{R} + \frac{1}{Ls} + Cs}\right]. \tag{16}$$

Figure 10 is the graph of Eq. (16) with $V(0) = 0$, $L = 7$ H, $R = 6, 8.57$ and $10.5\ \Omega$, $C = \frac{1}{42}$ F and $I(0) = 10$ A.

With considering Figs. 3 and 10 we can see that Eq. (16) with $V(0) = 0$ and $R = 6\ \Omega$ is equal to Eq. (9), which is the overdamped case. The critically damped case and the underdamped case are the results of Eq. (16) with resistance $8.57\ \Omega$ and $10.5\ \Omega$ and the initial zero voltage.

So Eq. (13) with $\alpha = 1$ and σ = non-zero is equal Eq. (15) and equal Eq. (16) with $V(0) = 60$, $L = 7$ H, $R = 6\ \Omega$, $C = \frac{1}{42}$ F and $I(0) = 10$ A.

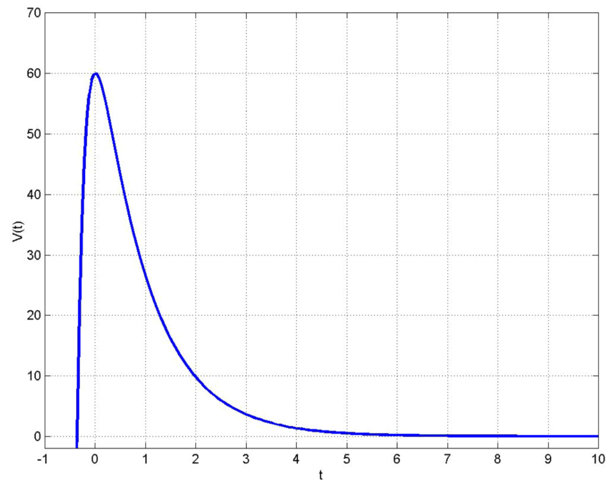

Figure 11 Graph of Eq. (16) with $V(0) = 60$ V, $L = 7$ H, $R = 6\ \Omega$, $C = \frac{1}{42}$ F and $I(0) = 10$ A

Case 2: in this case we want to replace the last term of (3) with the Caputo–Fabrizio fractional derivative and then apply the Laplace transform so we have

$$\begin{aligned}
&\frac{V}{R} + \frac{1}{L}\int_0^t V(p)\,dp - I(0) + \frac{C}{\sigma^{1-\alpha}}\mathcal{D}_t^\alpha V(t) = 0,\\
&\frac{1}{R}\mathcal{L}\big[V(t)\big] + \frac{1}{Ls}\mathcal{L}\big[V(t)\big] - \frac{I(0)}{s} + C\frac{s\mathcal{L}[V(t)] - V(0)}{\sigma^{1-\alpha}(s+\alpha(1-s))} = 0,\\
&\frac{1}{R}\mathcal{L}\big[V(t)\big] + \frac{1}{Ls}\mathcal{L}\big[V(t)\big] + \frac{Cs}{\sigma^{1-\alpha}(s+\alpha(1-s))}\mathcal{L}\big[V(t)\big] = \frac{I(0)}{s} + \frac{CV(0)}{\sigma^{1-\alpha}(s+\alpha(1-s))},\\
&\mathcal{L}\big[V(t)\big] = \frac{\frac{I(0)}{s} + \frac{CV(0)}{\sigma^{1-\alpha}(s+\alpha(1-s))}}{\frac{1}{R} + \frac{1}{Ls} + \frac{Cs}{\sigma^{1-\alpha}(s+\alpha(1-s))}}, \qquad (17)\\
&V(t) = \mathcal{L}^{-1}\left[\frac{\frac{I(0)}{s} + \frac{CV(0)}{\sigma^{1-\alpha}(s+\alpha(1-s))}}{\frac{1}{R} + \frac{1}{Ls} + \frac{Cs}{\sigma^{1-\alpha}(s+\alpha(1-s))}}\right]. \qquad (18)
\end{aligned}$$

Now we want to consider the graph of Eq. (18) with $V(0) = 0$.

Case 3: in Eq. (3) we replace the integration $\frac{1}{L}\int_0^t V(p)\,dp$ with Caputo–Fabrizio integration $I^\alpha V(t) = (1-\alpha)V(t) + \alpha\int_0^t V(p)\,dp$, $t \geq 0$, and the ordinary derivative with Caputo–Fabrizio fractional derivative so we have

$$\begin{aligned}
&\frac{1}{R}V(t) + \frac{1}{L}I^\alpha V(t) - I(0) + \frac{C}{\sigma^{1-\alpha}}\mathcal{D}^\alpha V(t) = 0,\\
&\frac{1}{R}V(t) + \frac{1-\alpha}{L}V(t) + \frac{\alpha}{Ls}\int_0^t V(p)\,dp - I(0) + \frac{C}{\sigma^{1-\alpha}}\mathcal{D}^\alpha V(t) = 0.
\end{aligned}$$

On applying the Laplace transform we have

$$\begin{aligned}
&\frac{1}{R}\mathcal{L}\big[V(t)\big] + \frac{1-\alpha}{L}\mathcal{L}\big[V(t)\big] + \frac{\alpha}{Ls}\mathcal{L}\big[V(t)\big] - \frac{I(0)}{s} + \frac{C}{\sigma^{1-\alpha}}\frac{(\mathcal{L}[V(t)] - V(0))}{(s+\alpha(1-s))} = 0,\\
&\mathcal{L}\big[V(t)\big]\left(\frac{1}{R} + \frac{1-\alpha}{L} + \frac{\alpha}{Ls} + \frac{Cs}{\sigma^{1-\alpha}(s+\alpha(1-s))}\right) = \frac{I(0)}{s} + \frac{CV(0)}{\sigma^{1-\alpha}(s+\alpha(1-s))},
\end{aligned}$$

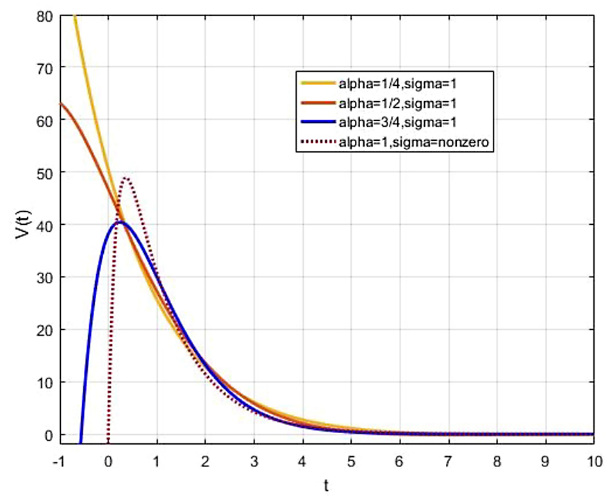

Figure 12 Graphs of Eq. (18) with $V(0) = 0$

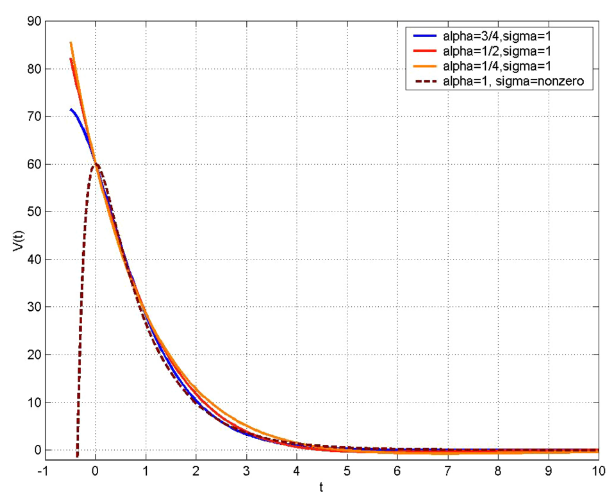

Figure 13 Graphs of Eq. (18) with $V(0) = 60$

$$\mathcal{L}\big[V(t)\big] = \frac{\frac{I(0)}{s} + \frac{CV(0)}{\sigma^{1-\alpha}(s+\alpha(1-s))}}{\frac{1}{R} + \frac{1-\alpha}{L} + \frac{\alpha}{Ls} + \frac{Cs}{\sigma^{1-\alpha}(s+\alpha(1-s))}}, \tag{19}$$

and applying the inverse Laplace transform then

$$V(t) = \mathcal{L}^{-1}\left[\frac{\frac{I(0)}{s} + \frac{CV(0)}{\sigma^{1-\alpha}(s+\alpha(1-s))}}{\frac{1}{R} + \frac{1-\alpha}{L} + \frac{\alpha}{Ls} + \frac{Cs}{\sigma^{1-\alpha}(s+\alpha(1-s))}}\right] \tag{20}$$

in Eq. (20) when $V(0) = 0$, then its graph is Fig. 15.

4 Some Note

Is it possible to fit the obtained data with some real data taken from the laboratory?

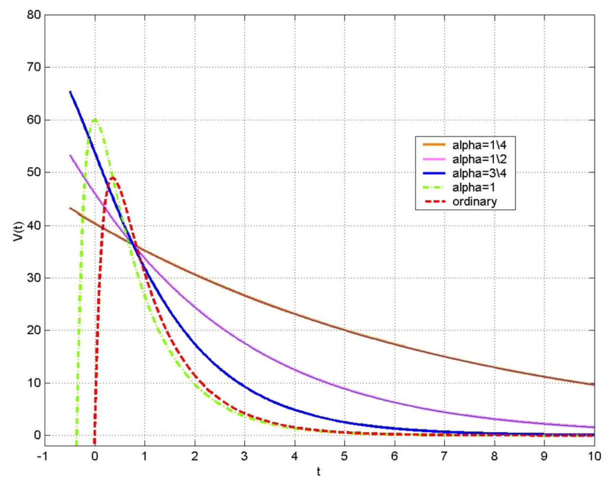

Figure 14 Graph of Eq. (20) with $V(0) = 60$ V

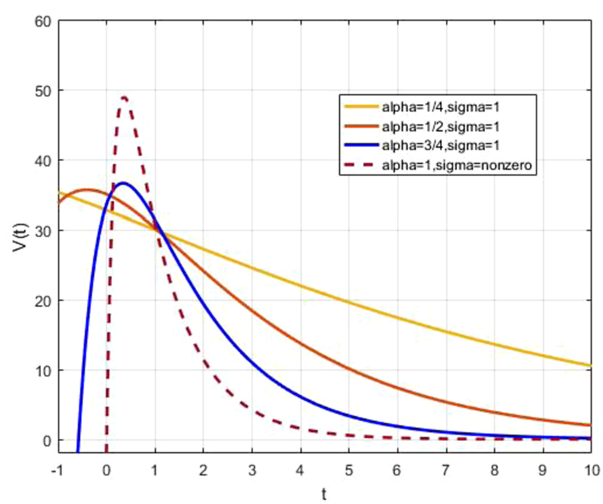

Figure 15 Graph of Eq. (20) with $V(0) = 0$

For this, as mentioned earlier, in most articles and books, the values used for the inductor and capacitor are relatively large (7 Henry for the inductor and 1/42 Farad for the capacitor) and the reason is to avoid working with negative powers of ten [3, 6, 9, 19, 27, 29, 33] However, it is not possible to study the transient parallel transmissions in very large quantities in the laboratory and in principle these very large amounts are not applicable in the real world, so we are looking for values that we can easily examine in the lab and we can examine in the software. For this work we used the schematics in Fig. 16.

The values of 900 micro-Henry for the inductor and 1 micro Farad for the capacitor and 10, 15 and 20 Ω for the resistance were selected for the overdamping, critical damping and underdamping modes. Measurement tools used in this project include Digital Oscilloscope GDS-1102B and digital Multimeters Victor VC9808 and DEC330FC and power supply PS-305D. FQPF10N20C N-Channel enhancement mode power field effect transis-

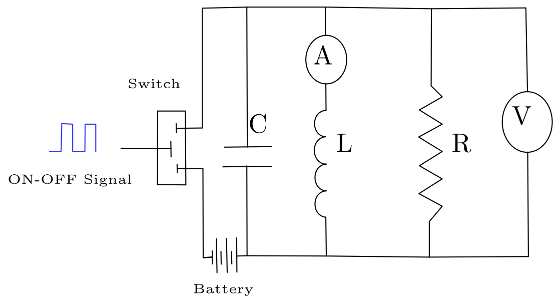

Figure 16 Schematic circuit used in the project

Figure 17 Details of switch signal

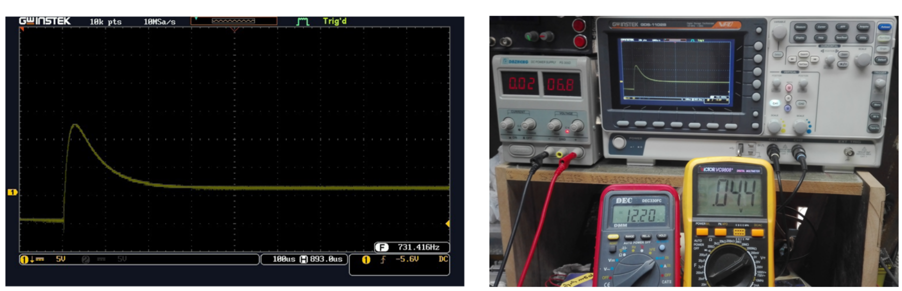

Figure 18 Overdamping mode measured values: $V = 44$ mV and $I = 12.2$ mA

tors with approximate frequency of 175 Hz and 8.8 percent Duty Cycle square signal were used (Fig. 17).

An oscilloscope with a sample rate of ten thousand points per second was used and the following results were obtained. For the overdamping mode the value of the voltage 44 mV and the current intensity 12.2 mA, for the critical damping mode the value of the voltage

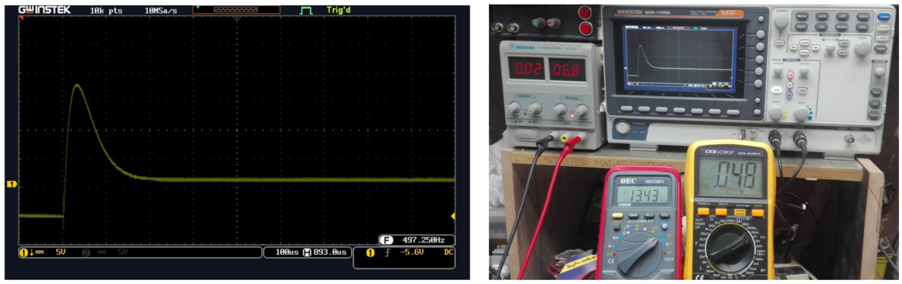

Figure 19 Critical damping mode measured values: $V = 48$ mV and $I = 13.43$ mA

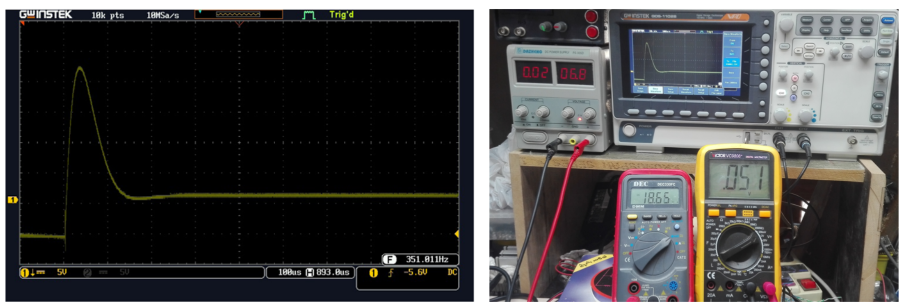

Figure 20 Underdamping mode measured values: $V = 51$ mV and $I = 18.65$ mA

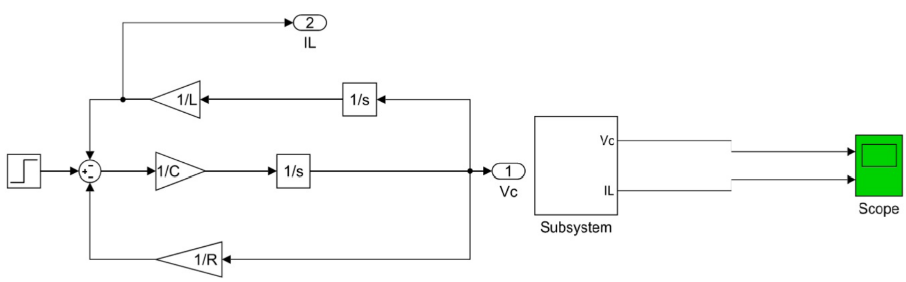

Figure 21 Solve Eq. (4) with MATLAB software

48 mV and the current intensity 13.43 mA and finally for the underdamping mode the value of the voltage 51 mV and the current intensity 18.65 mA were measured (Figs. 18, 19 and 20).

In the first simulation, we solve the differential Eq. (4) with MATLAB software and plot its graph with the measured values and compare them with the graphs drawn by the oscilloscope to see how the simulation of MATLAB software matches the actual results.

According to Fig. 21, the following simulation results are obtained for the measured values (Fig. 22).

By comparing the outputs of the software with the outputs of the oscilloscope, the software simulation defects are observed in parts of the graphs in which the curvature is not smooth (Figs. 23, 24 and 25).

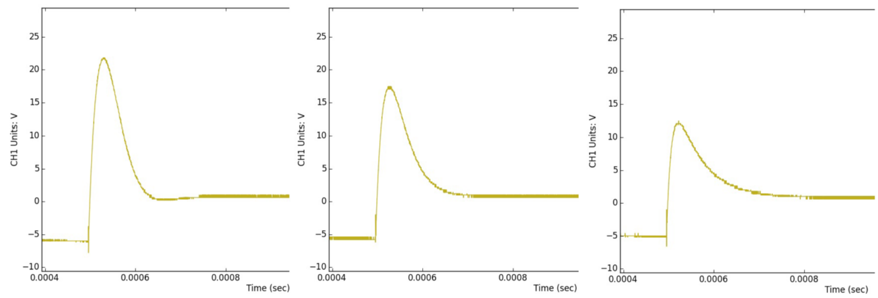

Figure 22 Outputs of oscilloscope

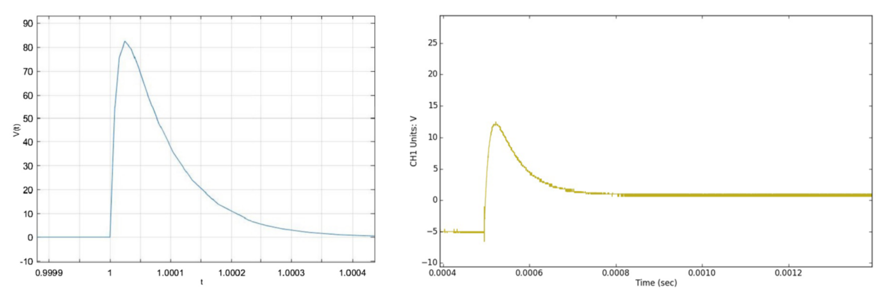

Figure 23 Overdamping mode comparison

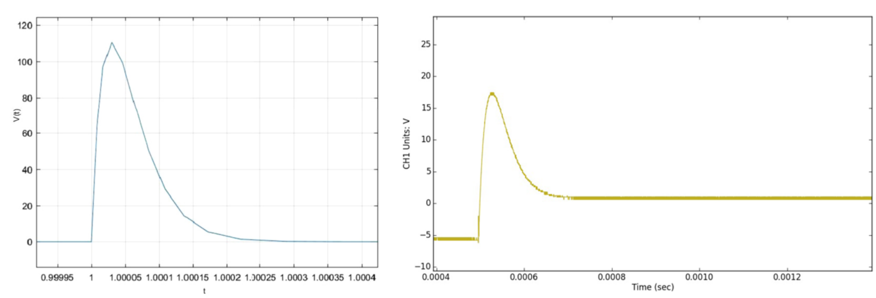

Figure 24 Critical damping mode comparison

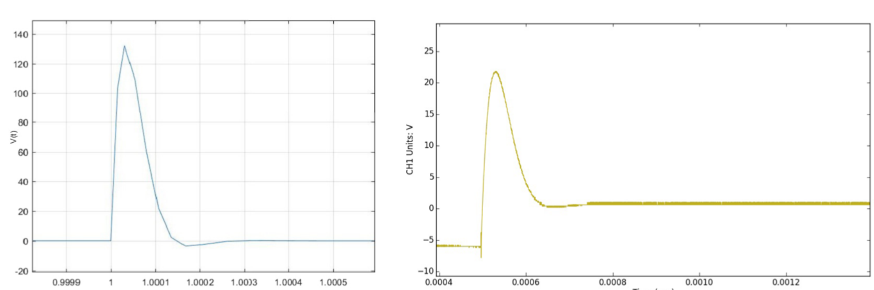

Figure 25 Underdamping mode comparison

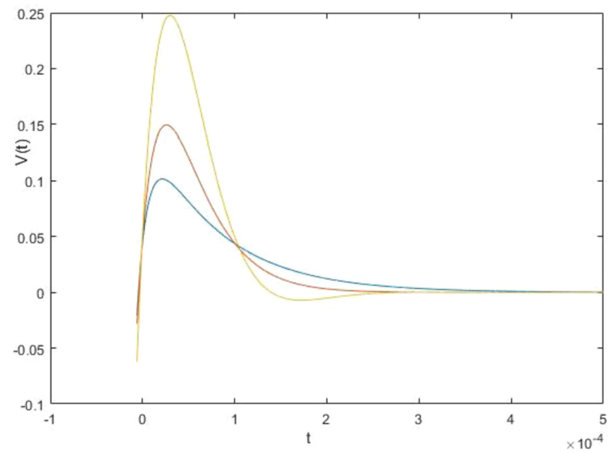

Figure 26 The graph of Eq. (4) for the values measured in the overdamping, critical damping and underdamping mode

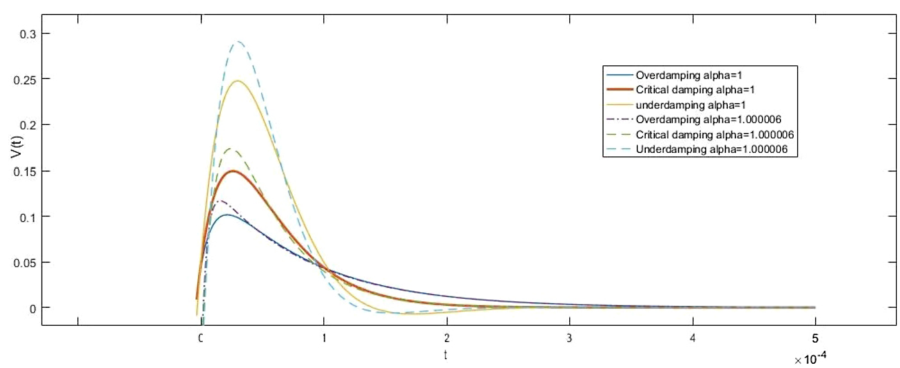

Figure 27 Comparison of the graphs of Eq. (18) for the measured values

To solve the problem of the unevenness of the curve in the previous simulation, we will use another simulation method. We intend to apply contrivance to obtain an acceptable match for the simulation output with an oscilloscope output for $\alpha = 1$ and then examine the simulation output behavior for less or more alpha values. In Fig. 26, Eq. (4) is plotted with the first simulation values using the plot command in MATLAB software.

By comparing the graph in Fig. 26 with the extracted oscilloscope graphs, the second simulation is more consistent. In the following, we will compare the graphs of Eqs. (18) and (20), in which the alpha is larger or smaller than 1, for the measured values, with Fig. 26.

With consideration of Figs. 27 and 29, we see that, with increasing alpha in Eqs. (18) and (20), the curves are narrower and taller than normal, and also shifted slightly to the right of the x-axis. In Figs. 28 and 30, by decreasing the alpha value, the curves are shorter and wider and slightly shifted to the left of the x-axis.

Also, the difference between Eqs. (18) and (20) is that in Eq. (20), the differences with the normal state are slightly greater than Eq. (18).

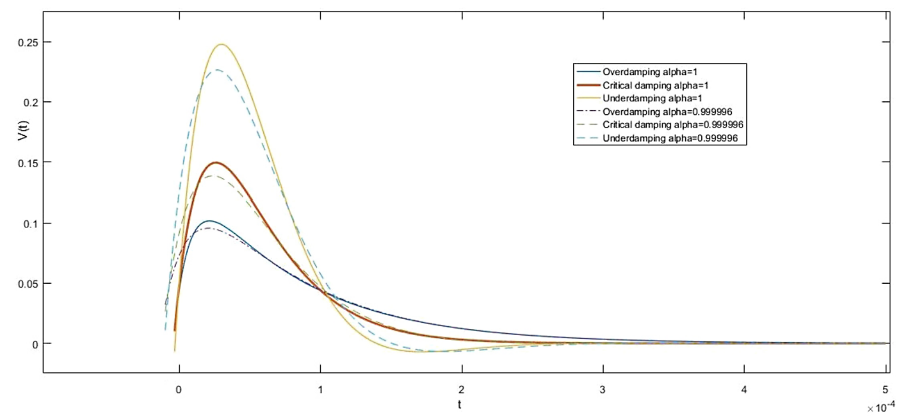

Figure 28 Comparison of the graphs of Eq. (18) for the measured values

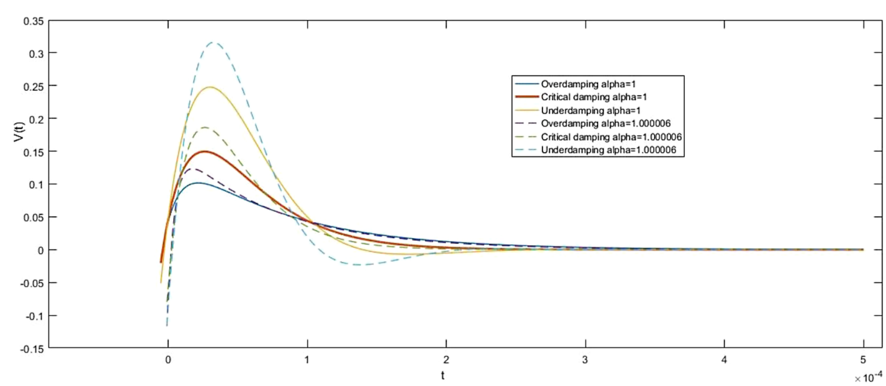

Figure 29 Comparison of the graphs of Eq. (20) for the measured values

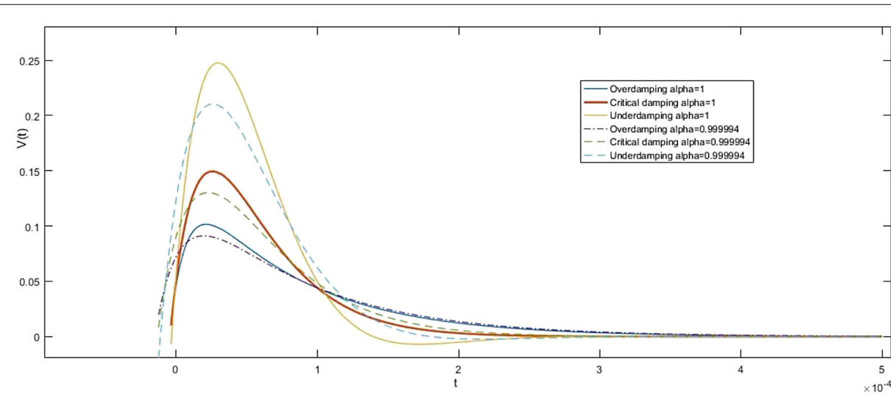

Figure 30 Comparison of the graphs of Eq. (20) for the measured values

Note For alpha values greater than 1.000006 and less than 0.999994, the transfer value of the curves to the right and left is much higher and eliminates the possibility of comparison with normal mode.

5 Conclusion

In order to find the transient response of the parallel RCL Circuit with Caputo–Fabrizio derivative and use of the inverse Laplace transformations when only the inductor has primary energy, it gives an obvious response, but it is used to find s_1 and s_2 in the equation $V(t) = A_1 e^{s_1 t} + A_2 e^{s_2 t}$.

When the capacitor also has primary energy, the transient response is obtained with the Laplace transforms and the inverse Laplace transformations. When σ takes values less than 1, the transient response curve is reduced. Most graphs are compared with each other when $\sigma = 1$. Of course, with $\alpha = 1$, the transient response in all states is identical to the transient response of the ordinary derivatives. To find the transient response of the parallel RCL circuit, the solution of Eq. (3) is much easier to find than Eq. (4).

The simulation part of MATLAB software did not perform well for laboratory values. By using the Caputo–Fabrizio fractional derivative with a derivative order slightly higher than 1, the voltage curve changes faster and with a larger amplitude. Conversely, with the use of the derivative of Caputo–Fabrizio with a derivative of less than 1, the curve changes the voltage more slowly and occurs with a smaller amplitude.

Question What is the physical interpretation of the Sigma with the opposite values 1?

Acknowledgements
The first and third authors were supported by Azarbaijan Shahid Madani University. The authors express their gratitude to the dear unknown referees for their helpful suggestions, which improved the final version of this paper.

Funding
Not applicable.

Availability of data and materials
Data sharing not applicable to this paper as no datasets were generated or analyzed during the current study.

Competing interests
The authors declare that they have no competing interests.

Authors' contributions
Each of the authors contributed to each part of this study equally and approved the final version of the manuscript.

Author details
[1]Department of Mathematics, Azarbaijan Shahid Madani University, Tabriz, Iran. [2]Department of Mathematics, Cankaya University, Ankara, Turkey. [3]Department of Medical Research, China Medical University Hospital, China Medical University, Taichung, Taiwan.

Publisher's Note

Springer Nature remains neutral with regard to jurisdictional claims in published maps and institutional affiliations.

Received: 19 October 2019 Accepted: 23 January 2020 Published online: 03 February 2020

References

1. Agarwal, R.P., Baleanu, D., Hedayati, V., Rezapour, S.: Two fractional derivative inclusion problems via integral boundary condition. Appl. Math. Comput. **257**, 205–212 (2015)
2. Alsaedi, A., Baleanu, D., Etemad, S., Rezapour, S.: On coupled systems of time-fractional differential problems by using a new fractional derivative. J. Funct. Spaces **2016**, Article ID 4626940 (2016)
3. Alsaedi, A., Nieto, J.J., Venktesh, V.: Fractional electrical circuits. Adv. Mech. Eng. **7**(12), 1687814015618127 (2015)
4. Atangana, A.: On the new fractional derivative and application to nonlinear fishers reaction–diffusion equation. Appl. Math. Comput. **273**, 948–956 (2016)
5. Atangana, A.: Non validity of index law in fractional calculus, a fractional differential, operator with Markovian and non-Markovian properties. Phys. A, Stat. Mech. Appl. **505**, 688–706 (2018)
6. Atangana, A., Alkahtani, B.S.T.: Extension of the resistance, inductance, capacitance electrical circuit to fractional derivative without singular kernel. Adv. Mech. Eng. **7**(6), 1687814015591937 (2015)
7. Atangana, A., Gómez-Aguilar, J.F.: Decolonisation of fractional calculus rules: breaking commutativity and associativity to capture more natural phenomena. Eur. Phys. J. Plus **133**(4), 166 (2018)

8. Atangana, A., Gómez-Aguilar, J.F.: Fractional derivatives with no-index law property: application to chaos and statistics. Chaos Solitons Fractals **114**, 516–535 (2018)
9. Atangana, A., Nieto, J.J.: Numerical solution for the model of RLC circuit via the fractional derivative, without singular kernel. Adv. Mech. Eng. **7**(10), 1687814015613758 (2015)
10. Aydogan, M.S., Baleanu, D., Mousalou, A., Rezapour, S.: On high order fractional integro-differential equations including the, Caputo–Fabrizio derivative. Bound. Value Probl. **2018**(1), 90 (2018)
11. Aydogan, S.M., Baleanu, D., Mousalou, A., Rezapour, S.: On approximate solutions for two higher-order Caputo–Fabrizio fractional, integro-differential equations. Adv. Differ. Equ. **2017**(1), 221 (2017)
12. Baleanu, D., Ghafarnezhad, K., Rezapour, S.: On a three step crisis integro-differential equation. Adv. Differ. Equ. **2019**(1), 153 (2019)
13. Baleanu, D., Güvenç, Z.B., Tenreiro Machado, J.A., et al.: New Trends in Nanotechnology and Fractional Calculus Applications. Springer, New York (2010)
14. Baleanu, D., Mousalou, A., Rezapour, S.: A new method for investigating approximate solutions of some fractional integro-differential equations involving the Caputo–Fabrizio derivative. Adv. Differ. Equ. **2017**(1), 51 (2017)
15. Baleanu, D., Mousalou, A., Rezapour, S.: On the existence of solutions for some infinite coefficient-symmetric, Caputo–Fabrizio fractional integro-differential equations. Bound. Value Probl. **2017**(1), 145 (2017)
16. Baleanu, D., Mousalou, A., Rezapour, S.: The extended fractional Caputo–Fabrizio derivative of order $0 \leq \sigma < 1$ on $C_{\mathbb{R}}[0,1]$ and the existence of solutions for two higher-order series-type differential equations. Adv. Differ. Equ. **2018**, 255 (2018)
17. Baleanu, D., Rezapour, S., Mohammadi, H.: Some existence results on nonlinear fractional differential equations. Philos. Trans. R. Soc., Math. Phys. Eng. Sci. **371**(1990), 20120144 (2013)
18. Baleanu, D., Rezapour, S., Saberpour, Z.: On fractional integro-differential inclusions via the extended fractional, Caputo–Fabrizio derivation. Bound. Value Probl. **2019**(1), 79 (2019)
19. Çalik, A.E., Şirin, H., Ertik, H., Şen, M.: Analysis of charge variation in fractional order LC electrical circuit. Rev. Mex. Fis. **62**(5), 437–441 (2016)
20. Caputo, M., Fabrizio, M.: A new definition of fractional derivative without singular kernel. Prog. Fract. Differ. Appl. **1**(2), 1–13 (2015)
21. Chauhan, J.P., Shah, P.V., Jana, R.K., Shukla, A.K.: Analytic solution for RLC circuit of non-integer order. Ital. J. Pure Appl. Math. **36**, 819–826 (2016)
22. Dumitru, B., Kai, D., Enrico, S.: Fractional Calculus: Models and Numerical Methods, vol. 3. World Scientific, Singapore (2012)
23. Dumitru, B., Khadijeh, G., Shahram, R., Mehdi, S.: On the existence of solutions of a three steps crisis integro-differential, equation. Adv. Differ. Equ. **2018**(1), 135 (2018)
24. Gómez Aguilar, J.F.: Behavior characteristics of a cap-resistor memcapacitor and a memristor from the response obtained of RC and RL electrical circuits described by fractional differential equations. Turk. J. Electr. Eng. Comput. Sci. **24**(3), 1421–1433 (2016)
25. Gómez Aguilar, J.F., Baleanu, D.: Solutions of the telegraph equations using a fractional calculus approach. Proc. Rom. Acad., Ser. A **15**, 27–34 (2014)
26. Gómez, F., Rosales, J., Guía, M.: RLC electrical circuit of non-integer order. Open Phys. **11**(10), 1361–1365 (2013)
27. Gómez-Aguilar, J., Morales-Delgado, V., Taneco-Hernández, M., Baleanu, D., Escobar-Jiménez, R., Al-Qurashi, M.: Analytical solutions of the electrical RLC circuit via Liouville–Caputo operators with local and non-local kernels. Entropy **18**(8), 402 (2016)
28. Gómez-Aguilar, J.F., Córdova-Fraga, T., Escalante-Martínez, J.E., Calderón-Ramón, C., Escobar-Jiménez, R.F.: Electrical circuits described by a fractional derivative with regular kernel. Rev. Mex. Fis. **62**(2), 144–154 (2016)
29. Gómez-Aguilar, J.F., Dumitru, B.: Fractional transmission line with losses. Z. Naturforsch. A **69**(10–11), 539–546 (2014)
30. Gómez-Aguilar, J.F., Razo-Hernández, R., Granados-Lieberman, D.: A physical interpretation of fractional calculus in observables terms: analysis of the fractional time constant and the transitory response. Rev. Mex. Fis. **60**(1), 32–38 (2014)
31. Gómez-Aguilar, J.F., Rosales-García, J., Guía-Calderón, M. Razo-Hernández, J.R.: Fractional RC and LC electrical circuits. Ing. Investig. Tecnol. **15**(2), 311–319 (2014)
32. Gómez-Aguilar, J.F., Rosales-García, J.J., Bernal-Alvarado, J.J., Córdova-Fraga, T., Guzmán-Cabrera, R.: Fractional mechanical oscillators. Rev. Mex. Fis. **58**(4), 348–352 (2012)
33. Hayt, W.H., Kemmerly, J.E., Durbin, S.M.: Engineering Circuit Analysis, vol. 214. McGraw-Hill, New York (1978)
34. Jain, R., Ali, M.F., Sharma, M.: An application of fractional calculus in RLC circuit. Int. J. Innov. Res. Adv. Eng. **2**(2), 1–3 (2015)
35. Kojabad, E.A., Rezapour, S.: Approximate solutions of a sum-type fractional integro-differential equation, by using Chebyshev and Legendre polynomials. Adv. Differ. Equ. **2017**(1), 351 (2017)
36. Losada, J., Nieto, J.J.: Properties of a new fractional derivative without singular kernel. Prog. Fract. Differ. Appl. **1**(2), 87–92 (2015)
37. Majka, Ł., Klimas, M.: Diagnostic approach in assessment of a ferroresonant circuit. Electr. Eng. **101**(1), 149–164 (2019)
38. Shah, P.V., Patel, A.D., Salehbhai, I.A., Shukla, A.K.: Analytic solution for the electric circuit model in fractional order. Abstr. Appl. Anal. **2014**, Article ID 343814 (2014)